Prosurvival Factors Improve Functional Engraftment of Myogenically Converted Dermal Cells into Dystrophic Skeletal Muscle

Lindsey A. Muir,[1,2,*] Charles E. Murry,[3–7] and Jeffrey S. Chamberlain[1,8,9]

In Duchenne muscular dystrophy (DMD) and other muscle wasting disorders, cell therapies are a promising route for promoting muscle regeneration by supplying a functional copy of the missing dystrophin gene and contributing new muscle fibers. The clinical application of cell-based therapies is resource intensive, and it will therefore be necessary to address key limitations that reduce cell engraftment into muscle tissue. A pressing issue is poor donor cell survival following transplantation, which in preclinical studies limits the ability to effectively test the impact of cell-based therapy on whole muscle function. We, therefore, sought to improve engraftment and the functional impact of in vivo myogenically converted dermal fibroblasts (dFbs) using a prosurvival cocktail (PSC) that includes heat shock followed by treatment with insulin-like growth factor-1, a caspase inhibitor, a Bcl-XL peptide, a K_{ATP} channel opener, basic fibroblast growth factor, Matrigel, and cyclosporine A. Advantages of dFbs include compatibility with the autologous setting, ease of isolation, and greater proliferative potential than DMD satellite cells. dFbs expressed tamoxifen-inducible MyoD and carried a mini-dystrophin gene driven by a muscle-specific promoter. After transplantation into muscles of *mdx* mice, a 70% reduction in donor cells was observed by day 5, and a 94% reduction by day 28. However, treatment with PSC gave a nearly three-fold increase in donor cells in early engraftment, and greatly increased the number of donor-contributed muscle fibers and total engrafted area in transplanted muscles. Furthermore, dystrophic muscles that received dFbs with PSC displayed reduced injury with eccentric contractions and an increase in maximum isometric force. Thus, enhancing survival of myogenic cells increases engraftment and improves structure and function of dystrophic muscle.

Introduction

SKELETAL MUSCLE HAS a remarkable capacity for regeneration. Resident stem cells, called satellite cells, readily participate in this process and help maintain myofibers. However, skeletal muscle pathology can lead to higher susceptibility to contraction-induced injury and impaired regeneration [1]. In the severe and progressive muscle wasting disorder Duchenne muscular dystrophy (DMD), repeated cycles of muscle injury and regeneration lead to accumulation of fibrotic connective tissue and fatty deposits [2].

DMD is caused by mutations in the dystrophin gene and is an X-linked recessive disorder affecting about 1:3,500 males born. Clinical onset is typically before age 5, with loss of mobility in the early teens and cardiac or respiratory failure before 30 [2]. No effective treatments currently exist that halt the progression of DMD, although supportive clinical interventions have greatly increased lifespan, and experimental gene repair and replacement therapies have immense potential.

Cell-based therapies are a promising approach that can combine gene replacement with the potential for skeletal muscle regeneration, and can be used concurrently with other gene replacement or repair strategies [3]. A wide variety of cells have been tested for their ability to engraft in skeletal muscle, supply dystrophin, improve contractile properties, and participate in regeneration [4]. Patient-derived, or autologous cells are attractive due to better immunological compatibility than donor-derived cells, but autologous cells must be accessible and of sufficient quantity for feasible creation of a therapeutic cell population. They must also undergo

[1]Department of Neurology and [2]Molecular and Cellular Biology Program, University of Washington, Seattle, Washington.
[3]Center for Cardiovascular Biology, [4]Institute for Stem Cell and Regenerative Medicine, Departments of [5]Pathology, [6]Bioengineering, and [7]Medicine/Cardiology, University of Washington, Seattle, Washington.
Departments of [8]Biochemistry and [9]Medicine/Medical Genetics, University of Washington, Seattle, Washington.
*Current affiliation: Department of Pediatrics and Communicable Diseases, University of Michigan Medical School, Ann Arbor, Michigan.

genetic correction and are typically cultured before use. Viral-based methods, for example, use of self-inactivating lentiviral vectors, are common for gene replacement in autologous cells.

Previous work shows that lentiviral-modified dermal fibroblasts (dFbs) are viable candidates for autologous cell therapy; they are accessible and readily expand in culture, can be converted into the myogenic lineage in vivo, and engraft after syngeneic transplantation in dystrophic mouse muscle [5–7]. Delivery of cells into muscle remains an issue for most cell therapies, and with many cell types, engraftment has been insufficient to see improvements in whole muscle function. Both myoblasts and dFbs reach plateaus in engraftment at specific cell quantities and concentrations [7,8]. High-density injection protocols have been developed to address this issue, with some success in providing therapeutic benefit in human muscle [9,10].

However, the transplantation setting itself is a barrier to high engraftment, and each cell type may have a specific tolerance for hypoxia, low nutrient perfusion, tissue damage, and inflammatory responses from transplantation and underlying disease processes. Mouse studies have shown that the inflammatory and ischemic microenvironment following transplantation promotes necrosis and apoptosis for donor cells [8,11]. Indeed, in a variety of tissues large numbers of transplanted cells die within 24 h of transplantation [12–14]. In principle, preserving donor cells in this early time window should improve engraftment and maximize therapeutic efficacy for injection of a given cell quantity.

An effective method for preventing rapid cell death may be to supply factors in the injectate that combat necrosis and apoptosis [15]. In addition, preconditioning that tolerizes cells to stressors encountered during transplantation may promote cell survival [16–18]. Since injected cells receive multiple signals that can promote cell death, addressing a single pathway may not adequately protect cells [19,20]. We, therefore, sought to test whether a combination of prosurvival and antiapoptosis components in the cell injectate would effectively promote survival and engraftment of myogenically converted dFbs following transplantation into dystrophic skeletal muscle.

Components of our prosurvival cocktail (PSC) included Matrigel to prevent anoikis [21]), cyclosporine A to inhibit cell death by blocking the mitochondrial permeability transition pore [17], a Bcl-XL cell-permeant peptide to inhibit mitochondrial death pathways [22], the pan-caspase inhibitor benzyloxycarbonyl-Val-Ala-Asp(O-methyl)-fluoromethyl ketone (ZVAD) [23], insulin-like growth factor 1 (IGF-1) to activate Akt [24], and Pinacidil to open K_{ATP} channels and tolerize cells to ischemic stress [25]. Cells were additionally heat shocked [16] 1 day before transplantation and hosts were treated with subimmunosuppressive doses of cyclosporine A.

By quantitative real-time polymerase chain reaction (qPCR) to detect donor cells, we found a nearly three-fold increase in the number of myogenically converted dFbs when PSC was used during transplantation into dystrophic mdx^{4cv} muscles. Histological analysis of injected muscles confirmed these results and showed increased fiber number and total area engrafted with PSC. In testing whole muscle contractile properties of mdx^{4cv} muscles after transplantation of dFb + PSC, we found reduced contraction-induced injury and increased maximum isometric force over saline-injected mdx^{4cv} controls.

Materials and Methods

Animals and animal care

For hosts in transplantation experiments, we used the dystrophic mdx^{4cv} mouse model of DMD that have a point mutation resulting in a stop codon in exon 53 of the dystrophin gene, on the C57Bl/6 background [26,27]. Donor cells were derived from the miniDys-GFP/mdx^{4cv} (miniDys-GFP) mouse line that contains a mini-dystrophin-eGFP fusion protein cDNA driven by human alpha-skeletal actin regulatory elements on the mdx^{4cv} background [28]. Host mice were 4–8 weeks old, and donor and host were syngeneic. Physiology experiments included age-matched C57Bl/6 mice as wild-type controls. All mice were bred in-house, and all animal procedures were approved by the Institutional Animal Care and Use Committee of the University of Washington.

Tamoxifen preparation and dosage

After equilibrating to room temperature, tamoxifen (TAM, T5648; Sigma-Aldrich) was dissolved in 65°C preheated corn oil (Sigma-Aldrich) at 100 mg/mL, with heating to 56°C and vortexing frequently for several hours or until most of the TAM was dissolved. The solution was then diluted to 40 mg/mL in corn oil, and heated/vortexed until TAM was completely dissolved. The TAM solution was filter sterilized and aliquoted for storage at −20°C. Working solutions were prepared by diluting aliquots to 20 mg/mL in sterile corn oil. To induce myogenic conversion of dFbs in vivo, mice were treated with 100 mg/kg TAM per day by intraperitoneal injection for 5 days, beginning 1 day before cell transplantation.

Cells and culture conditions

Dermal cells were isolated as in Muir et al. [7] from the dermis of 2- to 3-day-old male and female miniDys-GFP mice and cryogenically frozen. Whole muscle mononuclear (WMM) cells were isolated as described [28] from 4-week-old miniDys-GFP mice and were transplanted immediately, without culturing.

Growth medium (GM) for dermal cells was Dulbecco's modified Eagle's Medium (DMEM) +1 0% fetal bovine serum +1% penicillin/streptomycin (P/S) +2 mM L-glutamine (Gibco), with 10 ng/mL basic fibroblast growth factor (bFGF, R&D Systems) supplemented once per day. For transplantations, dermal cells were thawed (day 3) and expanded in GM for 1 day. To enable in vivo conversion into myogenic cells, dermal cells were transduced (day 2) with the lentiviral vector carrying TAM-inducible MyoD (MyoD-ER(T), [7]) at a multiplicity of infection of 10, in the presence of 8 µg/mL polybrene in 1 mL GM for 10 min. The cell/virus solution was then plated at 30%–60% confluency in 10 mL GM per 15-cm plate.

The following day (day 1), the cells in the PSC treatment group were heat shocked with GM prewarmed at 43°C, and kept at 43°C for 30 min, after which the GM was refreshed and supplemented with 200 nM cyclosporine A (Bedford Laboratories). For initial qPCR experiments, cells in both groups (with and without PSC) were heat shocked. Cells were trypsinized (0.05%) on the day of transplantation (day 0) and resuspended in either PSC or Ham's F10 medium (Gibco) +15% horse serum (Thermo Scientific/Hyclone) +1 mM $CaCl_2$ +1% P/S.

Prosurvival cocktail

The PSC used in this study is based on the cocktail tested by Laflamme et al. [15] in cardiac tissue. Injectate consisted of cells plus 50% vol/vol growth factor-reduced Matrigel, 100 nM cyclosporine A, 50 nM Bcl-XL (Calbiochem), 100 μM ZVAD (Calbiochem), 100 ng/mL IGF-1 (Pepro-Tech), and 50 μM Pinacidil (Sigma). In addition to the previously published formulation, we added 25 ng/mL bFGF because of its ability to promote fibroblast and myoblast survival [29]. Mice receiving cells with PSC were treated with daily subcutaneous injections of 5 mg/kg cyclosporine A, a lower dose than is required for immunosuppression [30,31], beginning 1 day before and ending 7 days after transplantation. For initial qPCR experiments, mice receiving cells without PSC were given a single 5 mg/kg dose of cyclosporine A 1 day before cell transplantation.

Cell transplantations

dFbs were prepared for transplantation in PSC or Ham's F10 medium with 15% horse serum, 1 mM $CaCl_2$, 1% P/S, and 0.5 μg/mL bFGF, kept on ice for 30 min to 3 h, and aspirated into a 25 μL Gastight Hamilton syringe equipped with a 32-gauge needle. About 500,000 dFbs were transplanted into tibialis anterior (TA) muscles, and about 200,000 dFbs were transplanted into extensor digitorum longus (EDL) muscles.

We chose the EDL for its consistent results in ex vivo whole muscle contractile studies, without potential contribution from other muscles as is observed in testing the TA muscle in situ. Furthermore, although EDL injections are technically challenging, its small size increases the potential for a higher percentage area engrafted. Engrafted EDLs are therefore a viable model system in which to test improvements in whole muscle function with cell-based therapy.

WMM cells were isolated as described [28] from 4-week-old miniDys-GFP mice, and were injected at ∼600,000 cells per EDL muscle. Note that due to the method of injection and size of EDLs, minor leakage of cell suspensions was observed during the injections for virtually all muscles, thus cell counts for EDLs are approximate. After opening the skin, cells were transplanted by single injection along the length of muscles. By hand, needles were inserted into near the distal tendon, and pushed longitudinally through the muscle to just below the proximal tendon. Injections were performed concurrently with needle withdrawal. Mice were anesthetized with inhaled 1%–5% isoflurane in oxygen and treated with standard postoperative care.

Tissue processing

Transplanted muscles for qPCR were harvested and processed using the DNeasy Blood and Tissue Kit (Qiagen) according to the manual with the following adaptations. We used 2–3 columns per muscle, adhering to a maximum of 20 mg per column. Muscles were digested overnight at 37°C and DNA extracted the following day into a final pooled volume of 800 μL per muscle, eluting twice in 65°C pre-warmed elution buffer per column. This volume therefore served as a normalization parameter for host muscle mass. For sectioning, transplanted muscles were harvested and frozen in cassettes in optimal cutting temperature compound in liquid nitrogen-cooled isopentane. Cryosections were cut every 100 μm throughout each muscle.

Quantitative real-time PCR

A 5 μL sample of final processed eluate for each muscle was used in triplicate for TaqMan qPCR (Applied Biosystems) to quantify the number of donor cells present per volume of tissue-derived eluate. The number of donor cells was determined by detecting a sequence from the lentiviral transfer plasmid that was inserted into donor cell genomes upon transduction (LV2 probe and primer set, [32]) in the tissue eluate. These values were normalized to the calculated cell population average of lentiviral copies per cell (LV2 and genomic low-density lipoprotein receptor probe and primer sets), determined through a separate qPCR on DNA extracted from a reserved portion of the transplanted cells. TaqMan probe and primer sets are shown in Supplementary Table S1 (Supplementary Data are available online at www.liebertpub.com/scd).

Physiology

Mice were anesthetized with 300 mg/kg Avertin (2, 2, 2-Tribromoethanol in tert-Amyl alcohol diluted with saline), with additional doses as necessary to maintain anesthesia for the procedure. Contractile properties were measured as described [28]. Briefly, proximal and distal EDL tendons were tied with 5-0 silk suture in situ, then muscles were dissected and one tendon was tied to the lever arm of a servomotor and one to a force transducer.

Muscles were maintained in a 25°C bath of buffered mammalian Ringer's solution (121 mM NaCl, 5 mM KCl, 50 μM $MgCl_2 \cdot 6H_2O$, 40 μM NaH_2PO_4, 24 mM $NaHCO_3$, 1.8 mM $CaCl_2 \cdot 2H_2O$, 5.5 mM glucose) that was bubbled with 95% O_2/5% CO_2. One test tetanus at low frequency (100 Hz) was performed after securing the muscle onto the rig to confirm viability and intact suture knots. Muscle length was then adjusted to optimal length (L_o) for force development. Muscles were stimulated with a pulse duration of 2 ms, and a voltage that produced maximum twitch force. A stimulation frequency of 180 Hz for EDL muscles, with 300 ms duration, gave the maximum isometric tetanic force (P_o).

We tested the susceptibility of muscles to contraction-induced injury using six lengthening contractions. The muscles were set at L_o, activated maximally, and then stretched through a strain of 30% of L_o at a velocity of one fiber length/s and then returned at the same velocity to L_o, allowed a 10 s recovery period, then exposed to subsequent stretches of 30% each. Note that mdx^{4cv} and C57BL/6 muscles were equally affected by slight fatigue in this protocol with 10 s recovery beyond four contractions.

After contractile testing, muscles were trimmed to remove sutures and tendons, weighed, and frozen in liquid nitrogen-cooled isopentane for sectioning. The cross-sectional area (CSA) in cm^2 was calculated to determine specific force, based on the measurements of optimal muscle length L_o (mm), muscle mass (mg), a muscle density of 1.06 g/cm^2, and a fiber length to optimal length ratio of 0.44. The specific P_o (kN/m^2) was determined by dividing P_o (kN) by calculated CSA (m^2). The force deficit in the lengthening contraction protocol was assessed by expressing P_o (mN) measured after

each lengthening contraction as a percentage of P_o before injury. One transplanted muscle was excluded from contractile studies due to the suture knot slipping.

Statistical analyses

Statistics were done using GraphPad Prism version 6.01 for Windows. Differences between samples were evaluated by unpaired *t*-test with Welch's correction where appropriate and by comparison of slopes in linear regression models, and curves were fit with one-phase association. Error bars are plotted as one standard deviation and significance set at $\alpha = 0.05$, unless stated otherwise.

Results

Rapid death of transplanted dFbs is attenuated by PSC

To quantify donor cell survival after transplantation, we used qPCR to detect sequences present only in donor cells that were transduced with the MyoD-ER(T) lentiviral vector. Initial qPCR experiments on a reserved portion of transduced dFbs that were prepared for transplantation confirmed a population average of at least one lentiviral integration per cell (see section "Materials and Methods"). After transplantation, dFbs were detected in host TA muscles in mice either not treated (NT) or treated with TAM to induce myogenic conversion.

Cell numbers rapidly declined in the first few days, with 73% of the cells lost between days 1 and 5 and 94% of the cells lost by day 28 (Fig. 1A). Without myogenic conversion in the NT cohort, we found even fewer donor cells, with roughly half as many dFbs detected on day 1 compared with the TAM cohort (Fig. 1A, inset). NT muscles lost 82% of dFbs between days 1 and 5. We then tested addition of the PSC to cell preparation and transplantation conditions in TAM-treated mice. When compared with dFb alone, dFb +

PSC increased the number of donor cells present 7 days after transplantation by about three-fold (Fig. 1B).

PSC improves early engraftment in dystrophic TA muscles

To confirm qPCR results, TAs were transplanted with dFbs alone or with PSC, harvested after 7 days, cryosectioned, and immunostained to detect miniDys-GFP expressed by engrafted donor cells. We quantified engraftment in five sections taken at equal intervals spanning the highest engrafted area. The PSC group had a significantly higher average number of miniDys-GFP⁺ myofibers across all sections of all muscles, higher miniDys-GFP⁺ fibers in maximally engrafted sections, and higher average area engrafted (Fig. 2A–C). Image panels in Fig. 2A show the maximally engrafted sections for each muscle with dFb alone or dFb + PSC.

In addition, we found a greater diameter across engraftment sites for the PSC group (Fig. 2A, D). Coupled with the observation of a lower density of engrafted fibers in the PSC group (Fig. 2F), these data suggest greater lateral migration. Higher engraftment persisted over longer distances longitudinally in the PSC group, as the outermost of the five sections flanking the highest engrafted section had significantly more miniDys-GFP⁺ fibers (Fig. 2A, E).

PSC improves engraftment in dystrophic EDL muscles

As a model for whole muscle functional testing, we performed dFb transplantations in EDLs. Compared with EDL transplantations with dFb alone, dFb + PSC had greater number of engrafted fibers when averaged across all seven sections flanking the highest engrafted section (Fig. 3A) and had more frequent sections with high levels of engraftment (Fig. 3B, C), consistent with TA data. We also estimated overall averages of fiber sizes by comparing measured
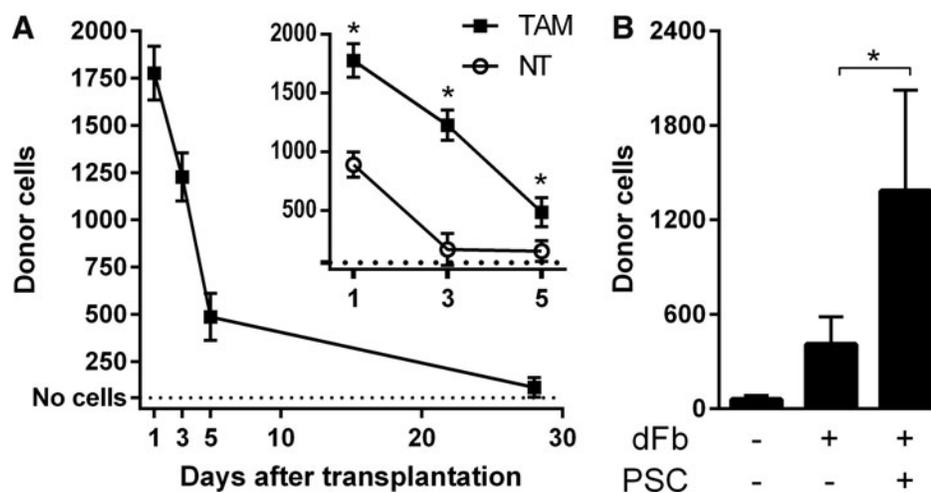

FIG. 1. Rapid loss of dFbs after transplantation is attenuated with PSC. **(A)** Donor dFbs detected by qPCR at multiple time points after transplantation. *Inset*, a comparison of dFbs in hosts that were either treated with TAM to induce myogenic conversion, or NT. Note that the early time point data shown in the inset for the group receiving TAM are the same as in the main graph. $n = 3$–5 per group. **(B)** Donor dFbs detected by qPCR 7 days after transplantation in the absence or presence of PSC. $n = 5$–8 per group. dFb, dermal fibroblast; qPCR, quantitative real-time polymerase chain reaction; TAM, tamoxifen; NT, not treated; PSC, prosurvival cocktail.
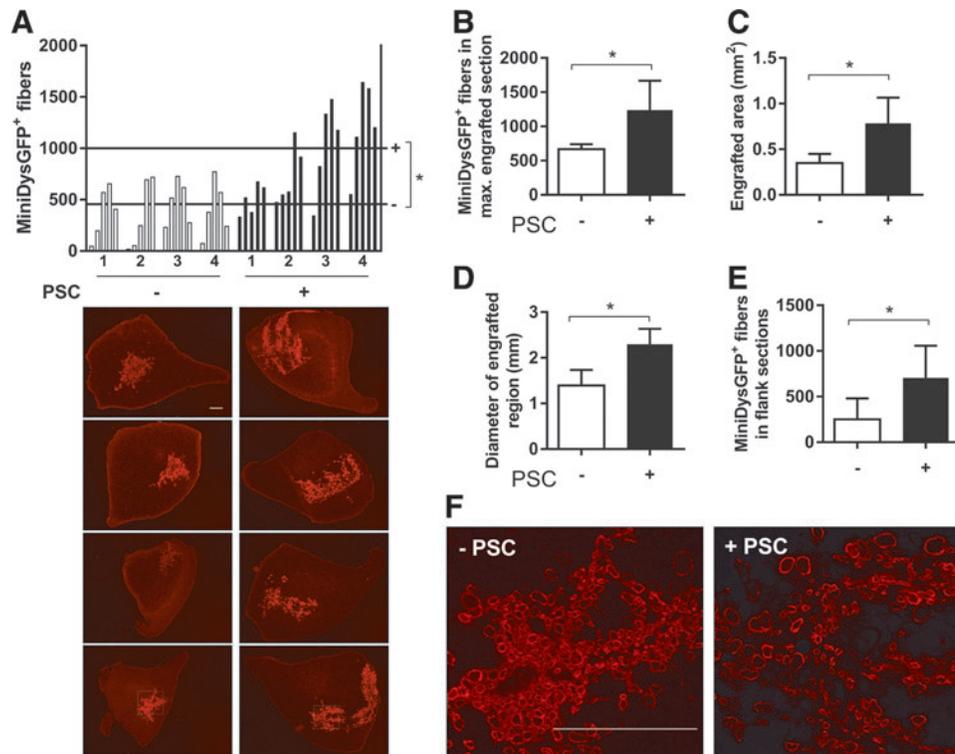
FIG. 2. PSC increases early engraftment in TA muscle fibers. **(A)** *Top*, TA engraftment profiles showing counts of miniDys-GFP[+] muscle fibers 7 days after transplantation with dFbs with or without PSC treatment. For each of four muscles per cohort, the number of fibers per section was counted across five sections every 700 μm through the muscles. *Horizontal lines* across the graph represent the average number of fibers per cohort, across all sections. *Bottom*, sections with maximum engraftment for each of four muscles per cohort are shown. **(B)** A comparison of the fiber counts in the maximum engrafted sections per muscle for each cohort. **(C)** A comparison of the areas in the maximum engrafted sections per muscle for each cohort. **(D)** A comparison of the diameters across the maximum engrafted sections per muscle for each cohort. **(E)** Longitudinal engraftment is shown by averaging fiber counts in the outermost sections flanking the maximum engrafted section for each cohort. **(F)** Higher magnification images of engrafted fibers for each cohort, of regions outlined in the *bottom panels* of **(A)**. *P < 0.05. Scale bars = 400 μm. TA, tibialis anterior.

engrafted area to the number of fibers engrafted. In engrafted sections, we found a higher frequency of small fibers and a lower frequency of larger fibers with PSC (Fig. 3D).

When engrafted area versus number of miniDys-GFP[+] fibers per section was plotted, the slope of the regression line for the PSC cohort was greater than the cohort without PSC (Fig. 3E). This supports that for a given engrafted area, more transgene-positive fibers were present when cells were injected with PSC. We observed that this effect was more pronounced in the PSC condition for more densely engrafted areas. Furthermore, the standard error of the model or variation in fiber number for a given engrafted area, captured by $S_{y.x}$, was much greater with dFb + PSC ($S_{y.x} = 123$) compared with dFb alone ($S_{y.x} = 50$), suggesting greater variability in fiber size.

Finally, with dFb + PSC, 60% of the transplanted EDLs had peak engraftment above 20% of the section (Table 1), a level of engraftment that has been associated with improvement in the dystrophic phenotype [33,34]. However, only 20% of the EDLs transplanted with dFbs alone reached this level. Furthermore, the peak-engrafted section for the dFb + PSC group was 51%, compared with 30% for dFb alone.

We observed high variability across engrafted muscles, as illustrated by engraftment profiles showing engrafted fiber counts and percentage area across seven sections per mus-

cle (Fig. 4A). Figure 4B exemplifies low, medium, and high engraftment observed in EDLs after immunofluorescence staining for GFP. To further assess the level of whole muscle engraftment, we estimated the absolute and percentage volume engrafted, determined by the product of the average percentage area engrafted or absolute area engrafted across all seven sections, and the total longitudinal distance engrafted for each muscle (Fig. 4C, D). We found that an average of 14% of the EDL was engrafted by volume, corresponding to an absolute volume of about 2 mm[3].

When we measured midbelly CSA across engrafted EDLs, we observed that the muscles that had the lowest engraftment had lower midbelly CSA (Fig. 4E). We then compared CSAs for engraftment levels of dFb + PSC above and below the 50th percentile (2 mm[3]), and indeed the highly engrafted group had significantly higher CSAs (Fig. 4F).

To explore whether cell injection increases CSA, we compared midbelly CSAs of saline-injected mdx^{4cv} EDLs to that of age-matched mdx^{4cv} muscles either injected with WMM cells or dFbs with and without PSC (Fig. 4G). dFb-transplanted muscles, with and without PSC, had significantly higher CSAs than controls. Interestingly, the greatest difference was observed for EDLs with the highest number of engrafted fibers, in the dFb + PSC group. Of note, muscle mass and length
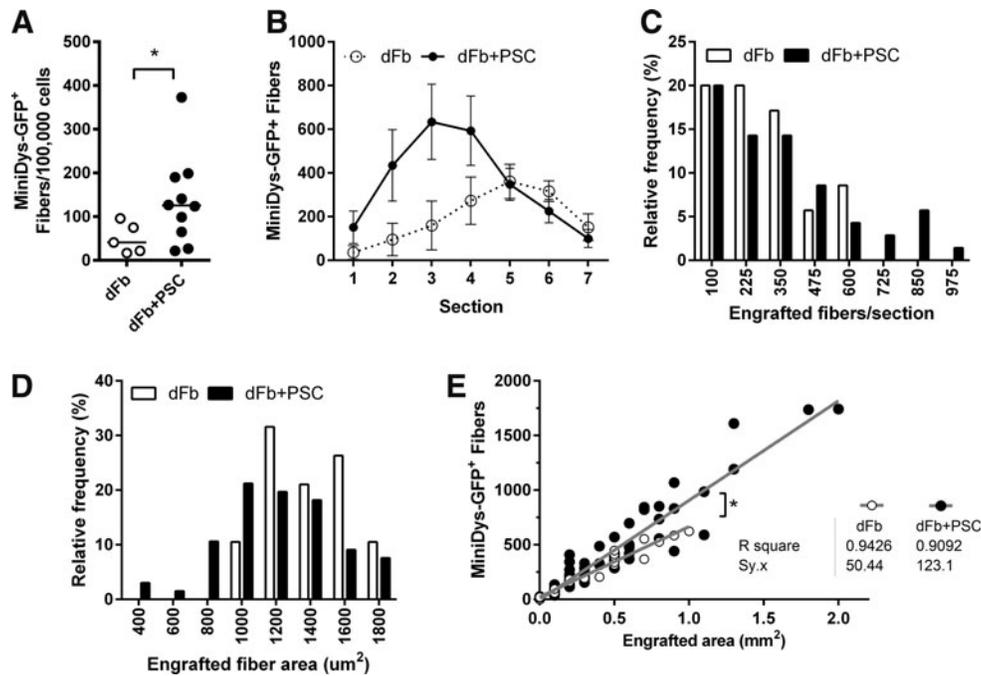
FIG. 3. PSC improves dFb engraftment in EDL muscles. **(A)** Number of miniDys-GFP[+] fibers per 100,000 cells injected, averaged across seven sections for each muscle with 700 μm between sections, 10 weeks after transplantation with dFb alone or dFb + PSC. *Lines* show the median. **(B)** Number of miniDys-GFP[+] fibers across seven sections for each cohort. Counts for each section are shown as mean ± standard error of the means. **(C)** Frequency distributions comparing the number of engrafted fibers per section between cohorts. Numbers on the *x*-axis represent bin centers, with the highest bin including frequencies of all engrafted counts above 975 fibers. **(D)** Frequency distribution comparing areas of individual engrafted fibers between cohorts. Numbers on the *x*-axis represent bin centers, with the highest bin including the frequencies of all engrafted fiber areas above 1,800 μm[2]. **(E)** Scatterplot comparing engrafted area versus number of miniDys-GFP[+] fibers for each cohort. *Gray lines* show linear regressions that capture differences in fiber number per area. *$P < 0.01$ for the difference in the slopes of regression lines. $n = 5$–10 per group. EDL, extensor digitorum longus.

were similar across control and dFb-injected muscles (Fig. 5C, F), so CSA differences were not attributable to overall size variation in muscles between cohorts.

To evaluate the relationship between engraftment and CSA at finer resolution, we plotted dFb + PSC-engrafted fiber number or area versus CSA in individual sections across all muscles. It is likely that the ends of EDLs did not receive sufficient exposure to cells with the injection method used. To avoid the confounding influence of low cell exposure at smaller CSA EDL ends, for each muscle only the three equidistant sections flanking the midbelly were studied.

TABLE 1. MEASURES OF PEAK ENGRAFTMENT
IN EXTENSOR DIGITORUM LONGUS TRANSPLANTED
WITH DERMAL FIBROBLASTS ALONE OR DERMAL
FIBROBLASTS + PROSURVIVAL COCKTAIL

	dFb		dFb + PSC	
Measure	*%*	*No.*	*%*	*No.*
Muscles with peak engraftment above 20%	20	1/5	60	6/10
Area (%) engrafted, peak in cohort	30	NA	51	NA

PSC, prosurvival cocktail; dFb, dermal fibroblast; NA, not applicable.

Engraftment had a significant positive nonlinear correlation with CSA for both fiber number and area, although a slightly greater correlation was found for fiber number (fiber number: Spearman $r = 0.704$, area: Spearman $r = 0.589$, Fig. 4H, I). While a similar trend increase in CSA for WMM-engrafted muscles was found ($P = 0.063$), no correlation was found between WMM engraftment levels and CSA (Fig. 4G and data not shown). Taken together, our data suggest that increases in CSA may occur locally with high engraftment levels and correspond to an increase in fiber number.

Transplantation of dFbs with PSC reduces injury with eccentric contractions

Previous testing of EDLs transplanted with dFbs or WMM without PSC showed no improvements in force and no protection from injury after eccentric contractions [7]. Here, dFb + PSC-transplanted EDLs were tested ex vivo to determine whether cell injections improved dystrophic muscle contractile properties.

Figure 5A shows the percentage of total force remaining after each of six lengthening contractions designed to induce injury. Transplanted muscles had significantly higher force remaining from contractions 4 to 6, compared with age-matched mdx^{4cv} controls (Fig. 5A, B). Supplementary Figure S1 shows the force decline for individual transplanted
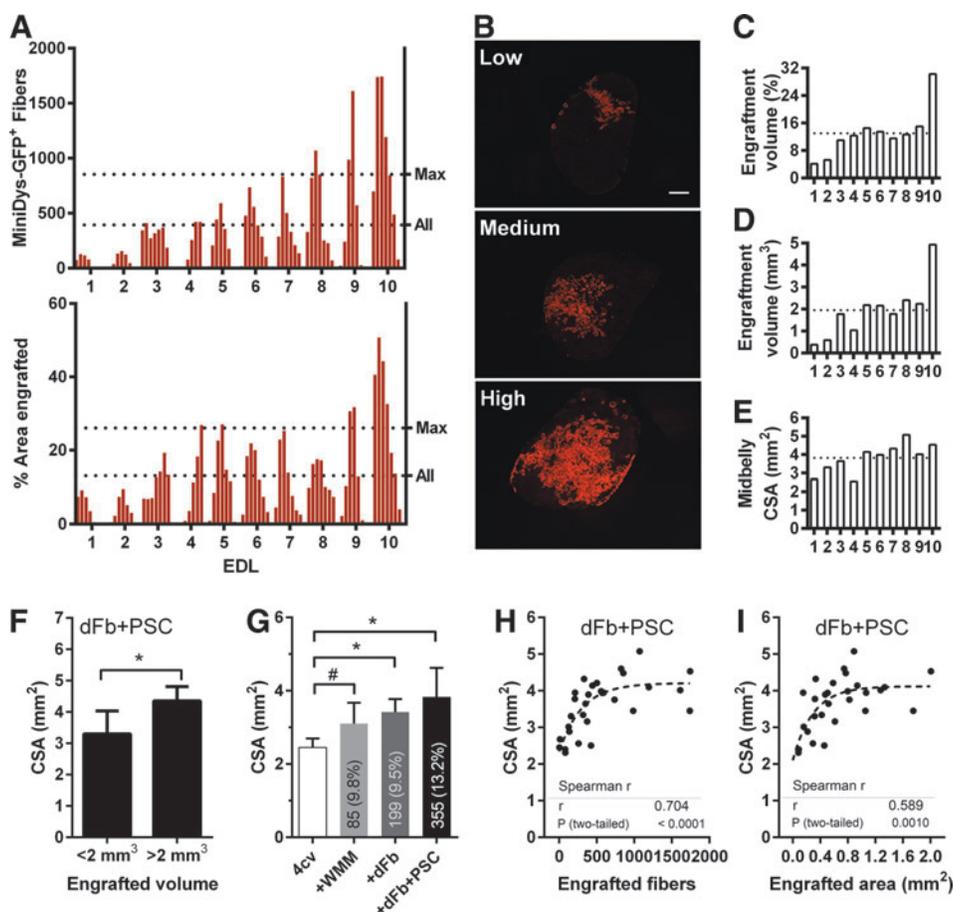
FIG. 4. Highly engrafted EDLs have greater CSA. **(A)** Engraftment across individual EDL muscles after dFb transplantation with PSC, with seven sections for each muscle and 700 μm between sections. The *dotted line* labeled Max was the average across all 10 muscles of the maximum engrafted sections. The *dotted line* labeled All was an average across all seven sections of all muscles. *Top*, number of miniDys-GFP$^+$ fibers in each section. *Bottom*, percentage area engrafted in each section. **(B)** EDL sections showing mini-DysGFP$^+$ fibers with immunofluorescence staining against GFP (*red*). Maximally engrafted sections for three EDLs exemplify the low, medium, and high engraftment observed in individual muscles. **(C)** The percentage volume engrafted in each EDL. **(D)** The absolute volume engrafted in each EDL. **(E)** The measured midbelly CSA of each muscle. **(C–E)** The *dotted line* represents the average across all muscles. **(F)** For dFb + PSC in EDLs, CSA for engrafted volume above or below the 50th percentile volume of 2 mm^3. **(G)** Midbelly CSAs for saline-injected EDLs compared with EDLs injected with WMM or dFbs with or without PSC. Text within bars shows the average number of engrafted fibers across transplanted muscles in each cohort, with the average percentage area of engraftment in parentheses. $n = 4$–10 per group; $^\#P = 0.063$. **(H, I)** Scatterplots of engrafted area or engrafted fibers versus CSA, in individual sections of EDL muscles transplanted with dFb + PSC. *Dotted lines* represent fitted curves illustrating nonlinearity in the data. $*P < 0.05$. CSA, cross-sectional area; WMM, whole muscle mononuclear cells.

muscles after each eccentric contraction. Transplanted and control muscles were no different in length at optimal force production and thus underwent equivalent stretching (Fig. 5C). Compared with controls, dFb-transplanted muscles had significantly higher maximum isometric force (Fig. 5D). We found no significant differences in specific force or mass, and both groups remained significantly different from wild type (Fig. 5E, F).

Discussion

Rapid loss of dFbs is consistent with other studies of fibroblasts and myoblasts after transplantation into muscle [12,35,36]. The more rapid loss of transplanted dFbs in the NT group compared with myogenically converting dFbs may be due to differential tolerance to transplantation stress, a feature also noted among different myogenic cell populations [37], or a survival advantage associated with activation of a myogenic program. This finding also suggests that if unconverted dFbs are present after TAM treatment, they are cleared from the muscle.

The addition of PSC to dFbs clearly improved cell survival and engraftment after transplantation. We observed higher donor cell numbers in the PSC condition by qPCR at 1 week posttransplantation and confirmed improved engraftment in TA and EDL muscles. The initial qPCR screen, in which all cells were heat shocked, showed that the PSC boosted cell survival beyond the effect of heat shock alone. Thus, use of multiple measures to combat apoptosis and necrosis is likely more effective than a single approach. The

FIG. 5. Engraftment of dFbs with PSC reduces injury with eccentric contractions. **(A)** Response of dFb + PSC-transplanted EDL muscles to six eccentric contractions, compared with control mdx^{4cv} and C57BL/6 (WT) muscles. **(B)** Bar graph representation of the responses of transplanted and control EDLs after the fifth eccentric contraction. **(C–F)** Comparisons of optimal length for force production (L_o), maximum isometric force, specific force, and mass of EDL muscles among cohorts. $n = 4–9$ muscles per group. WT, wild type.
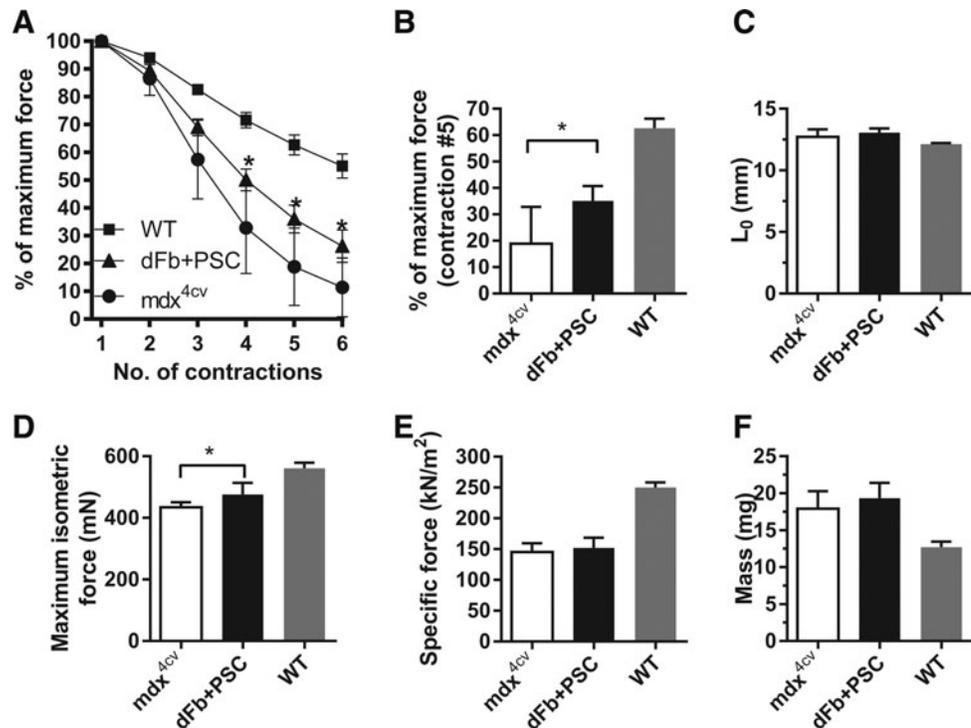
influence of PSC on proliferation of transplanted dFbs and on host muscle itself could also contribute to higher engraftment, including repair of the injection site, given the known physiological role of factors such as bFGF and IGF-1 in the growth, regeneration, and differentiation of skeletal muscle [29,38,39].

Compared with dFbs alone, we observed more small engrafted fibers in the PSC condition (Fig. 3C, D). Coupled with the finding that higher engrafted sections are associated with local increases in CSA, data suggest that PSC promoted donor-engrafted de novo fiber formation. However, these small fibers are likely developmentally immature, and as in the previous work we detected developmental myosin heavy chain in the majority of small-caliber donor cell-engrafted fibers [6]. The increase in CSA with cell injections may also reflect tissue remodeling that is not due to needle track injury alone, since all muscles received injections. Data also suggest that there is both a minimum level of engraftment required for increased CSA, and that CSA does not continue to increase beyond an upper threshold (Fig. 4H, I).

Evaluation of whole EDL contractile properties after transplantation of dFbs with PSC revealed slightly higher maximum isometric force in dFb-transplanted muscles, with no change in specific force or mass. Coupled with protection from contraction-induced injury, these data suggest that dFb engraftment can improve function in dystrophic muscle. Other studies have collected similar data after transplantation of myogenic cells. Improvements are not always observed despite engraftment, and in some cases improved contractile properties have been reported despite a low percentage of engrafted fibers in whole muscle [40–45].

These discrepancies highlight the many variables influencing improvements in dystrophic muscle after cell transplantation. These include cell origin, donor-contributed dystrophin levels, overall engrafted volume and distribution of engrafted fibers, engraftment variability, and de novo formation of myofibers. Further investigation of engraftment sites might greatly improve our understanding of how engrafted fibers contribute to force development, and help us to identify additional engraftment characteristics that associate with improved whole muscle function.

Specific methods used to assess contractile properties also differ across studies. While single engrafted myofiber isolation and physiology provides valuable information about fiber structure and expressed transgene localization [43], whole muscle contractile function must also be understood to assess the impact of the many interactions among engrafted and nonengrafted myofibers and potentially donor-derived de novo myofibers [33]. Understanding these features will be important for developing cell therapies that protect and improve function in dystrophic muscle.

Various other methods have been investigated for their potential to promote survival and engraftment of cells during transplantation. Injected cell suspensions rely on perfusion from existing vasculature, so it follows that implantation of large cell masses into muscle lowers viability and results in necrotic central regions [8]. Using fewer cells per injection improves survival, and using multiple injections can be used to increase transplanted cell numbers and circumvent migration issues [9,46]. Alternatively, promigratory factors can aid distribution of cells and thereby potentiate improvements in muscle function [47,48].

Other approaches for reducing cell death address oxidative stress, and include promoting activation of HIF-1, culturing cells in physiological rather than atmospheric oxygen levels, and conditioning with antioxidants [18,49,50]. Factors that stimulate angiogenesis could similarly combat hypoxia-induced death and promote skeletal muscle repair [51].

It is also important to consider the longevity of pro-survival effects when using cell populations that have

pluripotent origins [52], or have the potential to be transformed through previous genetic manipulations. For example, rAAV2-mediated expression of IGF-1 in myoblasts improves cell survival and stimulates angiogenesis [53]. However the long-term consequences of prolonged growth factor expression on transplanted or resident cells must be considered.

Indeed, Karvinen et al. show that long-term rAAV2-mediated expression of vascular endothelial growth factor promotes abnormal angiogenesis and fibrosis in rabbit skeletal muscle [54]. Alternatives that may prolong the activity of growth factors while avoiding permanent over-expression include cotransplantation of additional cells or bioscaffolds supplying factors that affect early survival of therapeutic cells, muscle repair, or angiogenesis [55,56].

Many of the required factors for a multipathway prosurvival approach could be adapted for use in a cell injectate in human clinical applications. Substrates to combat anoikis of injected cells could be produced from decellularization of autologous tissue biopsies [57]. For example, extracellular matrix from dermal tissue biopsies or even postmortem tissue [56] could be extracted and processed to provide a substrate for coinjection with transplanted cells. Substrates could also be derived from xenogeneic or synthetic origins, while keeping in mind specifications, such as elasticity and binding sites that preserve donor cell regenerative properties [57,58].

In summary, we have shown that multiple pathway-targeted PSC improves survival and engraftment of donor cells, in this study myogenically converted dFbs, a key step in improving cell therapies for skeletal muscle. Furthermore, dFbs injected with PSC into dystrophic muscle reduce injury from eccentric contractions. This study provides a useful framework for preclinical testing of cell populations for engraftment and functional benefit to skeletal muscle.

Acknowledgments

Author Disclosure Statement

J.S.C. is a member of the Scientific Advisory Boards of Solid GT, Sarepta Therapeutics, and Akashi Therapeutics.

References

1. Batchelor CL and SJ Winder. (2006). Sparks, signals and shock absorbers: how dystrophin loss causes muscular dystrophy. Trends Cell Biol 16:198–205.
2. Emery AE and F Muntoni. (2003). *Duchenne Muscular Dystrophy*. Oxford University Press, Oxford.
3. Muir LA and JS Chamberlain. (2009). Emerging strategies for cell and gene therapy of the muscular dystrophies. Expert Rev Mol Med 11:e18.
4. Bertoni C. (2014). Emerging gene editing strategies for Duchenne muscular dystrophy targeting stem cells. Front Physiol 5:148.
5. Vangipuram M, D Ting, S Kim, R Diaz and B Schule. (2013). Skin punch biopsy explant culture for derivation of primary human fibroblasts. J Vis Exp e3779.
6. Kimura E, JJ Han, S Li, B Fall, J Ra, M Haraguchi, SJ Tapscott and JS Chamberlain. (2008). Cell-lineage regulated myogenesis for dystrophin replacement: a novel therapeutic approach for treatment of muscular dystrophy. Hum Mol Genet 17:2507–2517.
7. Muir LA, QG Nguyen, SD Hauschka and JS Chamberlain. (2014). Engraftment potential of dermal fibroblasts following in vivo myogenic conversion in immunocompetent dystrophic skeletal muscle. Mol Ther Methods Clin Dev 1:14025.
8. Skuk D, M Paradis, M Goulet and J Tremblay. (2007). Ischemic central necrosis in pockets of transplanted myoblasts in nonhuman primates: implications for cell-transplantation strategies. Transplantation 84:1307–1315.
9. Skuk D, M Goulet, B Roy, V Piette, CH Cote, P Chapdelaine, J-Y Hogrel, M Paradis, J-P Bouchard, et al. (2007). First test of a ''high-density injection'' protocol for myogenic cell transplantation throughout large volumes of muscles in a Duchenne muscular dystrophy patient: eighteen months follow-up. Neuromuscul Disord 17:38–46.
10. Perie S, C Trollet, V Mouly, V Vanneaux, K Mamchaoui, B Bouazza, JP Marolleau, P Laforet, F Chapon, et al. (2014). Autologous myoblast transplantation for oculopharyngeal muscular dystrophy: a phase I/IIa clinical study. Mol Ther 22:219–225.
11. Huard J, R Roy, J Bouchard, F Malouin, C Richards and J Tremblay. (1992). Human myoblast transplantation between immunohistocompatible donors and recipients produces immune reactions. Transplant Proc 24:3049–3051.
12. Guérette B, D Skuk, F Célestin, C Huard, F Tardif, I Asselin, B Roy, M Goulet, R Roy, M Entman and JP Tremblay. (1997). Prevention by anti-LFA-1 of acute myoblast death following transplantation. J Immunol 159:2522–2531.
13. Snyder BR, AM Chiu, DJ Prockop and AWS Chan. (2010). Human multipotent stromal cells (MSCs) increase neurogenesis and decrease atrophy of the striatum in a transgenic mouse model for Huntington's disease. PLoS ONE 5: e9347.
14. Robey TE, MK Saiget, H Reinecke and CE Murry. (2008). Systems approaches to preventing transplanted cell death in cardiac repair. J Mol Cell Cardiol 45:567–581.
15. Laflamme MA, KY Chen, AV Naumova, V Muskheli, JA Fugate, SK Dupras, H Reinecke, C Xu, M Hassanipour, et al. (2007). Cardiomyocytes derived from human embryonic stem cells in pro-survival factors enhance function of infarcted rat hearts. Nat Biotechnol 25:1015–1024.
16. Laflamme MA, J Gold, C Xu, M Hassanipour, E Rosler, S Police, V Muskheli and CE Murry. (2005). Formation of human myocardium in the rat heart from human embryonic stem cells. Am J Pathol 167:663–671.
17. Nakagawa T, S Shimizu, T Watanabe, O Yamaguchi, K Otsu, H Yamagata, H Inohara, T Kubo and Y Tsujimoto. (2005). Cyclophilin D-dependent mitochondrial permeability transition regulates some necrotic but not apoptotic cell death. Nature 434:652–658.
18. Bartoszuk-Bruzzone U, A Burdzińska, A Orzechowski and Z Kłos. (2012). Protective effect of sodium ascorbate on efficacy of intramuscular transplantation of autologous muscle-derived cells. Muscle Nerve 45:32–38.

19. Mendell JR, JT Kissel, AA Amato, W King, L Signore, TW Prior, Z Sahenk, S Benson, PE McAndrew, et al. (1995). Myoblast transfer in the treatment of Duchenne's muscular dystrophy. N Engl J Med 333:832–838.

20. Hill E, T Boontheekul and DJ Mooney. (2006). Regulating activation of transplanted cells controls tissue regeneration. Proc Natl Acad Sci U S A 103:2494–2499.

21. Zvibel I, F Smets and H Soriano. (2002). Anoikis: road-block to cell transplantation? Cell Transplant 11:621–630.

22. Cao G. (2002). In vivo delivery of a Bcl-xL fusion protein containing the TAT protein transduction domain protects against ischemic brain injury and neuronal apoptosis. J Neurosci 22:5423–5431.

23. Montolio M, N Tellez, M Biarnes, J Soler and E Montanya. (2005). Short-term culture with the caspase inhibitor z-VAD.fmk reduces beta cell apoptosis in transplanted islets and improves the metabolic outcome of the graft. Cell Transplant 14:59–65.

24. Davis ME. (2006). Local myocardial insulin-like growth factor 1 (IGF-1) delivery with biotinylated peptide nanofibers improves cell therapy for myocardial infarction. Proc Natl Acad Sci U S A 103:8155–8160.

25. Ardehali H and B O'Rourke. (2005). Mitochondrial K(ATP) channels in cell survival and death. J Mol Cell Cardiol 39:7–16.

26. Chapman VM, DR Miller, D Armstrong and CT Caskey. (1989). Recovery of induced mutations for X chromosome-linked muscular dystrophy in mice. Proc Natl Acad Sci U S A 86:1292–1296.

27. Im WB, SF Phelps, EH Copen, EG Adams, JL Slightom and JS Chamberlain. (1996). Differential expression of dystrophin isoforms in strains of mdx mice with different mutations. Hum Mol Genet 5:1149–1153.

28. Li S, E Kimura, R Ng, BM Fall, L Meuse, M Reyes, JA Faulkner and JS Chamberlain. (2006). A highly functional mini-dystrophin/GFP fusion gene for cell and gene therapy studies of Duchenne muscular dystrophy. Hum Mol Genet 15:1610–1622.

29. Kinoshita I, J-T Vilquin and JP Tremblay. (1995). Pretreatment of myoblast cultures with basic fibroblast growth factor increases the efficacy of their transplantation in mdx mice. Muscle Nerve 18:834–841.

30. Batiuk TD, J Urmson, D Vincent, RW Yatscoff and PF Halloran. (1996). Quantitating immunosuppression. Estimating the 50% inhibitory concentration for in vivo cyclosporine in mice. Transplantation 61:1618–1624.

31. Aharoni R, A Yussim, M Sela and R Arnon. (2005). Combined treatment of glatiramer acetate and low doses of immunosuppressive drugs is effective in the prevention of graft rejection. Int Immunopharmacol 5:23–32.

32. Sastry L, T Johnson, MJ Hobson, B Smucker and K Cornetta. (2002). Titering lentiviral vectors: comparison of DNA, RNA and marker expression methods. Gene Ther 9:1155–1162.

33. Chamberlain JS. (1997). Dystrophin levels required for genetic correction of Duchenne muscular dystrophy. Basic Appl Myol 7:251–255.

34. Sharp PS, H Bye-a-Jee and DJ Wells. (2011). Physiological characterization of muscle strength with variable levels of dystrophin restoration in mdx mice following local antisense therapy. Mol Ther 19:165–171.

35. Lattanzi L, G Salvatori, M Coletta, C Sonnino, MG Cusella De Angelis, L Gioglio, CE Murry, R Kelly, G Ferrari, et al. (1998). High efficiency myogenic conversion of human fibroblasts by adenoviral vector-mediated MyoD gene transfer. An alternative strategy for ex vivo gene therapy of primary myopathies. J Clin Invest 101:2119–2128.

36. Fan Y, M Maley, M Beilharz and M Grounds. (1996). Rapid death of injected myoblasts in myoblast transfer therapy. Muscle Nerve 19:853–860.

37. Qu Z, L Balkir, JCT van Deutekom, PD Robbins, R Pruchnic and J Huard. (1998). Development of approaches to improve cell survival in myoblast transfer therapy. J Cell Biol 142:1257–1267.

38. Seed J and SD Hauschka. (1988). Clonal analysis of vertebrate myogenesis. VIII. Fibroblasts growth factor (FGF)-dependent and FGF-independent muscle colony types during chick wing development. Dev Biol 128:40–49.

39. Cornelison DDW, MS Filla, HM Stanley, AC Rapraeger and BB Olwin. (2001). Syndecan-3 and syndecan-4 specifically mark skeletal muscle satellite cells and are implicated in satellite cell maintenance and muscle regeneration. Dev Biol 239:79–94.

40. Rousseau J, N Dumont, C Lebel, SP Quenneville, CH Côté, J Frenette and JP Tremblay. (2010). Dystrophin expression following the transplantation of normal muscle precursor cells protects mdx muscle from contraction-induced damage. Cell Transplant 19:589–596.

41. Mueller GM, T O'Day, J Watchko and MP Ontell. (2002). Effect of injecting primary myoblasts versus putative muscle-selved stem cells on mass and force generation in mdx mice. Hum Gene Ther 13:1081–1090.

42. Cerletti M, S Jurga, CA Witczak, MF Hirshman, JL Shadrach, LJ Goodyear and AJ Wagers. (2008). Highly efficient, functional engraftment of skeletal muscle stem cells in dystrophic muscles. Cell 134:37–47.

43. Tedesco FS, MFM Gerli, L Perani, S Benedetti, F Ungaro, M Cassano, S Antonini, E Tagliafico, V Artusi, et al. (2012). Transplantation of genetically corrected human iPSC-derived progenitors in mice with limb-girdle muscular dystrophy. Sci Transl Med 4:140ra89.

44. Darabi R, RW Arpke, S Irion, JT Dimos, M Grskovic, M Kyba and RC Perlingeiro. (2012). Human ES- and iPS-derived myogenic progenitors restore DYSTROPHIN and improve contractility upon transplantation in dystrophic mice. Cell Stem Cell 10:610–619.

45. Darabi R, K Gehlbach, RM Bachoo, S Kamath, M Osawa, KE Kamm, M Kyba and RCR Perlingeiro. (2008). Functional skeletal muscle regeneration from differentiating embryonic stem cells. Nat Med 14:134–143.

46. Pellegrini K and M Beilharz. (2011). The survival of myoblasts after intramuscular transplantation is improved when fewer cells are injected. Transplantation 91:522–526.

47. Lafreniere J-F, M-C Caron, D Skuk, M Goulet, AR Cheikh and JP Tremblay. (2009). Growth factor coinjection improves the migration potential of monkey myogenic precursors without affecting cell transplantation success. Cell Transplant 18:719–730.

48. Bentzinger CF, J von Maltzahn, NA Dumont, DA Stark, YX Wang, K Nhan, J Frenette, D Cornelison and MA Rudnicki. (2014). Wnt7a stimulates myogenic stem cell motility and engraftment resulting in improved muscle strength. J Cell Biol 205:97–111.

49. Wu Y, J Wu, DY Lee, A Yee, L Cao, Y Zhang, C Kiani and BB Yang. (2005). Versican protects cells from oxidative stress-induced apoptosis. Matrix Biol 24:3–13.

50. Liu W, Y Wen, P Bi, X Lai, XS Liu, X Liu and S Kuang. (2012). Hypoxia promotes satellite cell self-renewal and

enhances the efficiency of myoblast transplantation. Development 139:2857–2865.

51. Bouchentouf M, BF Benabdallah, P Bigey, TM Yau, D Scherman and JP Tremblay. (2008). Vascular endothelial growth factor reduced hypoxia-induced death of human myoblasts and improved their engraftment in mouse muscles. Gene Ther 15:404–414.

52. Cunningham JJ, TM Ulbright, MF Pera and LHJ Looijenga. (2012). Lessons from human teratomas to guide development of safe stem cell therapies. Nat Biotechnol 30:849–857.

53. Subramanian IV, BC Fernandes, T Robinson, J Koening, KS Lapara and S Ramakrishnan. (2009). AAV-2-mediated expression of IGF-1 in skeletal myoblasts stimulates angiogenesis and cell survival. J Cardiovasc Transl Res 2:81–92.

54. Karvinen H, E Pasanen, TT Rissanen, P Korpisalo, E Vahakangas, A Jazwa, M Giacca and S Yla-Herttuala. (2011). Long-term VEGF-A expression promotes aberrant angiogenesis and fibrosis in skeletal muscle. Gene Ther 18:1166–1172.

55. Saif J, TM Schwarz, DYS Chau, J Henstock, P Sami, SF Leicht, PC Hermann, S Alcala, F Mulero, et al. (2010). Combination of injectable multiple growth factor—releasing scaffolds and cell therapy as an advanced modality to enhance tissue neovascularization. Arterioscler Thromb Vasc Biol 30:1897–1904.

56. Briggs D and JE Morgan. (2013). Recent progress in satellite cell/myoblast engraftment—relevance for therapy. FEBS J 280:4281–4293.

57. Turner N and S Badylak. (2012). Regeneration of skeletal muscle. Cell Tissue Res 347:759–774.

58. Gilbert PM, KL Havenstrite, KEG Magnusson, A Sacco, NA Leonardi, P Kraft, NK Nguyen, S Thrun, MP Lutolf and HM Blau. (2010). Substrate elasticity regulates skeletal muscle stem cell self-renewal in culture. Science 329:1078–1081.

Address correspondence to:
Dr. Jeffrey S. Chamberlain
Department of Neurology, University of Washington
Seattle, WA 98195-7720

E-mail: jsc5@uw.edu